Runoff generation from a combined glacier and páramo catchment within the Antisana Reserve in Ecuador

Minaya, Veronica; Camacho Suarez, Vivian; Wenninger, Jochen; Mynett, Arthur

DOI
10.1080/24705357.2021.2005472

Publication date
2023

Document Version
Final published version

Published in
Journal of Ecohydraulics

Citation (APA)
Minaya, V., Camacho Suarez, V., Wenninger, J., & Mynett, A. (2023). Runoff generation from a combined glacier and páramo catchment within the Antisana Reserve in Ecuador. *Journal of Ecohydraulics*, *8*(2), 192-207. https://doi.org/10.1080/24705357.2021.2005472

JOURNAL OF ECOHYDRAULICS
2023, VOL. 8, NO. 2, 192–207
https://doi.org/10.1080/24705357.2021.2005472

Taylor & Francis
Taylor & Francis Group

Runoff generation from a combined glacier and *páramo* catchment within the Antisana Reserve in Ecuador

Veronica Minaya[a], Vivian Camacho Suarez[b], Jochen Wenninger[c] and Arthur Mynett[c,d]

[a]Department of Civil and Environmental Engineering, Escuela Politecnica Nacional, Quito, Ecuador; [b]Civil Engineering Department, University of Sheffield, Sheffield, UK; [c]Department of Water Science and Engineering, UNESCO-IHE Institute for Water Education, Delft, the Netherlands; [d]Section of Hydraulic Engineering, Delft University of Technology, Delft, the Netherlands

ABSTRACT

Runoff processes in glacier and *páramo* catchments in the Andean region are of interest as they are vitally important to serve the water needs of surrounding communities. Particularly in Northern Ecuador, the runoff processes are less well-known due to the high variability of precipitation, young volcanic ash soil properties, soil moisture dynamics and other local factors. Previous studies have shown that the melting of glaciers contributes to runoff generation and that the *páramo* ecosystem plays an important role in regulating runoff during periods of low precipitation. Data collection and experimental investigations were carried out in a catchment of 15.2 km^2 and altitude ranging between 4000 and 5700 m above sea level. Environmental tracers and hydrochemical catchment characterization were used for identifying runoff sources and their respective contributions during dry and wet conditions. Dry conditions are defined as periods where precipitation was absent for at least three consecutive days and wet conditions imply rainfall events. This study highlights the importance of the *páramo* on contributing to total runoff during baseflow (70% of total runoff) and the capacity of the *páramo* to dissipate the stream energy and buffer the peak flow during rainfall conditions. Electrical conductivity together with stable isotopes were identified as conservative tracers that characterize the end-member concentrations.

ARTICLE HISTORY
Received 17 June 2021
Accepted 5 November 2021

KEYWORDS
Environmental tracers; runoff generation; water chemistry; *páramos*; tropical grasslands

Introduction

Tropical grasslands are one of the most abundant but probably least-understood ecosystems in terms of their biological and physical processes. In the Andean region such grasslands are known as *páramos* and they have been recognized for their importance in providing water for agriculture and urban use (Buytaert and Beven 2011), and sustaining biodiversity and unique ecological processes (Hofstede et al. 2002; Madriñán et al. 2013). The importance of the *páramos* is associated with the tremendous capacity of water retention in its volcanic ash soil covered by vegetation (Poulenard et al. 2002; Tonneijck 2009; Roa-García et al. 2011). Ecuador has nearly 12,500 km^2 of *páramo* of which 64% in areas above 3000 m a.s.l. has been transformed or degraded (Hofstede et al. 2002) and the remaining areas are currently under constant pressure. At a higher elevation (>4000 m a.s.l.), these ecosystems are influenced by permanent snow and glaciers that feed directly the river's drainage system or may contribute further downstream due to glacial meltwater infiltrations and water resurgence through springs (Favier et al. 2008; Villacis et al. 2008; Cauvy-Fraunié et al. 2013).

A lot of attention has been given on the relationship between climate change and retreating glaciers globally (Beniston 2003), particularly because climate change in conjunction with the rapid change in land use can jeopardize the water quantity and quality of the *páramos* (Jansky et al. 2002; Buytaert et al. 2006b; Buytaert and Beven 2009). Bradley et al. (2006) showed clear evidence of faster surface temperature changes in higher elevations compared to lower elevations in the Tropical Andes with a rate of 0.11 °C per decade in the period 1939–1998. The concern of the scientific community lies in the implications of the melting water and its impact on hydrological systems alongside the response of the terrestrial, aquatic biota (Cauvy-Fraunié et al. 2013) and water security for communities that rely on these catchments in the tropical regions (Brown et al. 2010; Kaser et al. 2010). The complexity of these glacierized *páramo* catchments is higher than those in temperate regions since *páramo* catchments are more affected by a continuous ablation at all elevations (Kaser and Osmaston 2002) leading to

CONTACT Veronica Minaya veronica.minaya@epn.edu.ec Department of Civil and Environmental Engineering, Escuela Politecnica Nacional, Ladrón de Guevara E11-253, P.O. Box 17-01-2759, Quito, Ecuador.

Supplemental data for this article is available online at https://doi.org/10.1080/24705357.2021.2005472

changes in the hydrological, geomorphic and ecological processes. Due to the orographic properties of these high mountainous regions in the *páramos*, the precipitation regime has a remarkably large spatial variability (Buytaert et al. 2006b; Celleri and Feyen 2009).

Several studies enhance the importance of a fair understanding of the hydrological complexity of these interconnected systems and the implications for water resources management in the region (Buytaert et al. 2010; Buytaert and Beven 2011; Viviroli et al. 2011; Cuesta et al. 2013; Carrillo-Rojas et al. 2016). Tracer experiments have been widely used to provide more information about the connectivity and time scales of the contribution of the main runoff sources and flow pathways to the total runoff (Huss et al. 2008; Villacis et al. 2008; Wenninger et al. 2008; Condom et al. 2012; Dahlke et al. 2012; Munyaneza et al. 2012; Windhorst et al. 2013). However, appropriate tracers for a suitable spatial hydrochemical characterization have not yet been identified. In addition, a quantification of the different contributions from glacier and *páramo* components in catchments of complex geology and topography remains a challenge.

This study aims to (i) identify effective environmental tracers (stable isotopes and major ions) to quantify the contribution of the main runoff components, and (ii) provide an understanding of the runoff generation of a glacierized *páramo* system during dry and wet conditions.

Study area

Location

The study catchment Los Crespos-Humboldt (15.2 km^2) lies within the Antisana Ecological Reserve (628.1 km^2) in the Andean region of Ecuador (Figure 1a). It is located at the south-western slope of the Antisana volcano (0°30′S, 78°11′W) and its elevation ranges from 4000 to 5700 m a.s.l (Figure 1b). This catchment is one of several water sources for La Mica reservoir that supplies water for the southern part of Quito, the capital city of Ecuador, located 50 km north of this catchment.

Land cover

It consists of 15% glaciers, 68% *páramo* grasslands and 17% moraines (Figure 1c,b). The latter one is an ecosystem in transition between the glacier and the *páramo*. The *páramo* vegetation is dominated by tussock grasses (*Calamagrostis intermedia*), acaulescent rosettes (*Werneria nubigena, Hypochaeris sessiliflora*) and cushions (*Azorella pedunculata*) (Minaya et al. 2016) (Figure 1c). The *páramo* vegetation has adapted to specific climatic conditions of low atmospheric pressure, high radiation and wind drying effects (Luteyn 1999). The glacier is an icecap that has retreated around 200 meters in the last 20 years (Cáceres et al. 2005; Hall et al. 2012).

Soil properties

The soils are andosols derived from volcanic material based on the FAO classification (Gardi et al. 2014). These are characterized by their high soil moisture (Buytaert et al. 2005a) and water retention capacity (Roa-García et al. 2011; Janeau et al. 2015). The soil texture influences the ecological and hydrological processes. Sandy soils drain well and reduce the capability of holding moisture; silty soils offer a high water-holding capacity. The slopes are moderate (up to 15°) at lower elevations and increase up to 30° close to the moraines at higher elevations.

Climate

From lower to higher elevations the precipitation in the catchment increases from 900 to 1200 mm/yr, with an average annual precipitation of 745 mm/yr to 993 mm/yr for the Humboldt (4010 m a.s.l.) and the Crespos (4785 m a.s.l.) weather stations, respectively. The average temperature ranges from 4.8 °C to 7.0 °C (for the period 2000 to 2011) for the same elevations. Figure 2 shows the climate diagram of monthly average values of precipitation and maximum and minimum temperatures at the two weather stations (Humboldt and Crespos) for the period of 2000 to 2011. The wet period extends typically from April to June. In the Ecuadorian Andes, the *páramos* above 3000 m a.s.l. receive 16% more precipitation compared to other *páramos* located in the inter-Andean valleys (Buytaert and Beven 2011). There are two main sources of precipitation: those influenced by the air masses from the Amazon region and those influenced by the inter-Andean valley regime (Vuille et al. 2000).

Precipitation has a large spatial variability (Buytaert et al. 2006a) with a presence of the so-called "horizontal precipitation", which consist of fog and mist developed from the orographic uplift caused by the Andes (Buytaert et al. 2005b), which also limits transpiration (Buytaert and Beven 2011). Although, this additional source of water is minor and mostly intercepted by arbustive vegetation (*Chuquiraga*), other studies (Crockford and Richardson 2000; Foot and Morgan 2005) showed that the *páramo* ecosystem can catch low energy rain, drizzle and fog moisture on their leaves, which conduct over 50% of rainwater directly to the

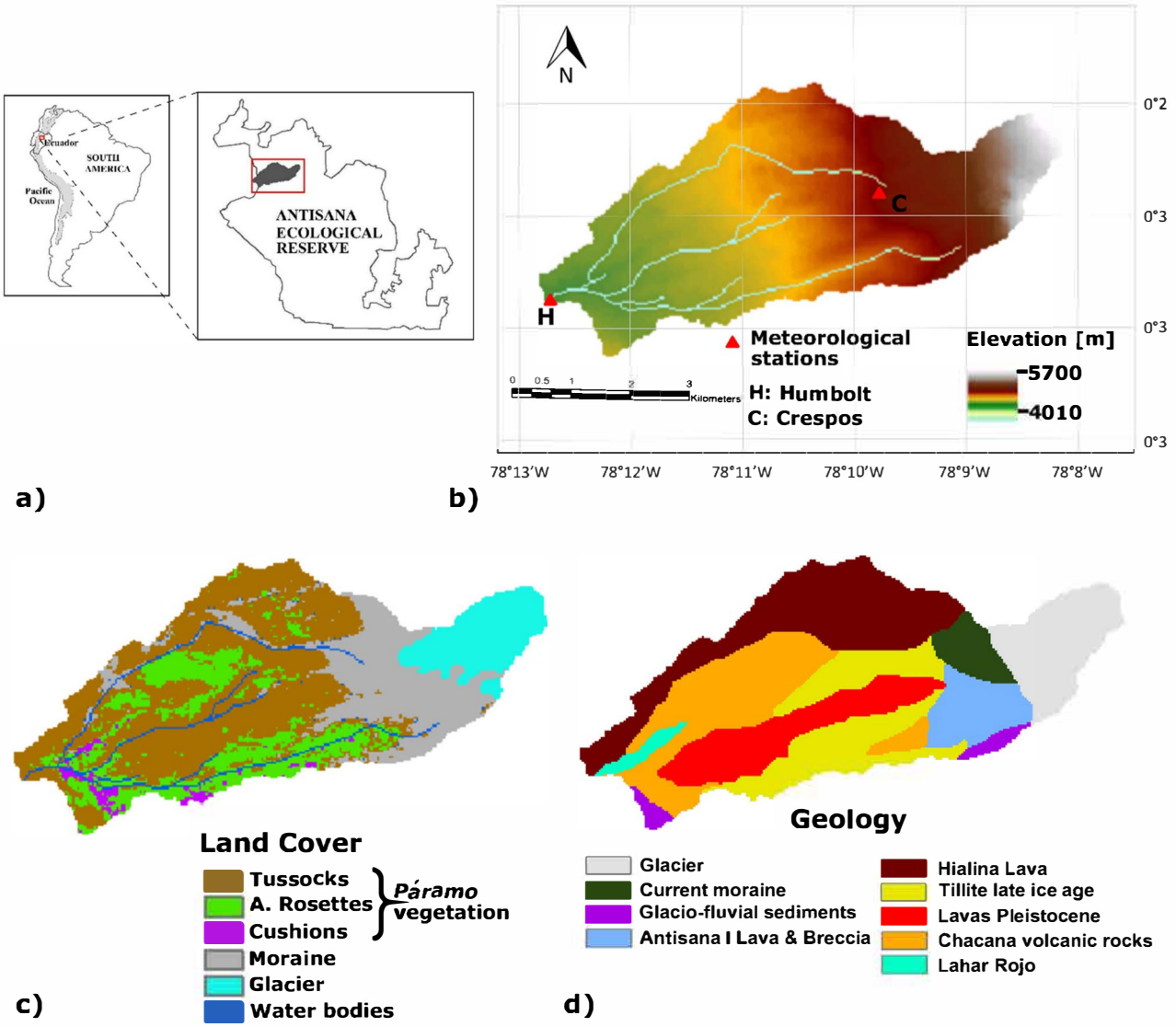

Figure 1. (a) Location of the Los Crespos-Humboldt basin within The Antisana Ecological Reserve, Ecuador; (b) Elevation of the catchment with the main stream network and location of the meteorological stations, (c) Land cover map (source: Minaya et al. 2016), and d) Geological background (source: Hall et al. 2012).

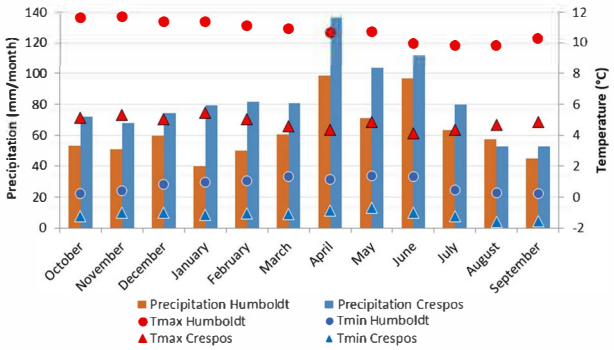

Figure 2. Average monthly precipitation, maximum and minimum average monthly temperatures at Humboldt and Crespos weather stations from 2000 to 2011.

volcanic ash soils of Ecuadorian highlands (Janeau et al. 2015).

Geology

The geology of the catchment has a wide detritic range that holds a variety of volcanic deposits from previous eruptions (Figure 1d). The last significant eruption in the Antisana occurred nearly 1000 years ago based on stratigraphic studies (Cáceres et al. 2005; Hall et al. 2012; 2017). The study area could have received ashes from different volcanoes as a result of an increase of eruptive frequency during the Holocene (Hall and Mothes 1999; Bernard and Andrade 2011). The peak is slightly flat; it presumes that the crater is glacier filling. Although there has not been volcanic activity or hot fumeroles lately, there are reports of SO_2 gas in higher elevations (Cáceres et al. 2005; Hall et al. 2012). Most of the stratigraphy is composed of dark layers of ash and andesite scoria, which is a product of the fall of eruptive clouds with intercalations of fluvial deposits (Cáceres et al. 2005; Hall et al. 2012).

The geology as shown in Figure 1d is composed of the glacier, moraines, glacial-fluvial sediments, tillites, volcanic rocks and Lahar rojo. The moraines are deposited debris that form along the glacier due to the receding of the glacier. These areas are

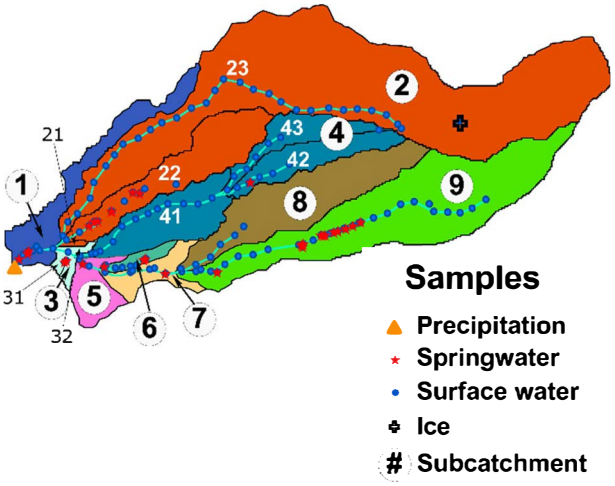

Figure 3. Subcatchment division with sampling locations for precipitation, spring water, surface water and ice.

characterized by lagune formations which intercept meltwater. The Lavas Pleistocene formation is older volcanic pyroclastic deposits which are composed of andesite rocks containing plagioclase, amphibole and feldspar minerals (Hall et al. 2012). The Hialina Lava is formed also of andesite content; however, this is a younger formation with olivine, plagioclase and quartz, arranged in a matrix formed by volcanic glass (Alvarado 2009). The Lahar Rojo is a sequence of red volcanic lava deposits along the Antisana river. Its pyroclastic material when mixed with water became red indicating several volcanic eruptions during the Holocene.

Data and methods

Data collection

The catchment is equipped with two hydro-meteorological stations (Figure 1b) managed by the National Institute of Meteorology and Hydrology of Ecuador (INAMHI). The DEM that was used has a resolution of 20 m x 20 m and was obtained from the contour line drawings from the Ecuadorian Military Geographical Institute (IGM) at a scale 1:50,000. The stream network was based on a 'hydrological approach' as defined by Mark (1984) and Lo and Yeung (2007) and later verified during ground-truthing recording GPS point measurements and field observations. The subcatchment delineation was created using the multiple flow direction model (Tarboton 1997) and the eight-direction method (D8) introduced by O'Callaghan and Mark (1984). The station located at the outlet of the catchment is the Humboldt station (4010 m a.s.l.), which records data of precipitation, water levels, temperature and electrical conductivity of the water. Isotopic and hydrochemical samples were collected in a sampling campaign carried out in July 2014. Samples were collected during dry conditions on July 4–7 and during wet conditions on July 14–15. Figure 3 shows the catchment with the sampling sites. The catchment contains two main tributaries that originate from the Antisana glacier. Catchments # 4, 5, 6, 7, 8 and 9 flow through *páramo* vegetation and from now on will be referred to as *páramo* catchment. Catchment #2 flows through large boulders and rocks of different size on a mixed catchment of water coming directly from the glacier (subcatchment 23) without any other type of contribution until it meets a small tributary of a combined source of surface and spring water (subcatchment 22). Subcatchment 23 from now on will be referred to as glacier catchment.

The highest monthly average flow during the year occurs in June, with an average of 300 l s^{-1}; whereas the lowest monthly flow occurs in March with an average of 200 l s^{-1}. Due to the technical and logistics limitations in the study area, flow was measured only at the outlet of the catchment. Precipitation was also monitored at the outlet of the catchment.

Experimental set-up

During dry conditions

In this study, dry conditions are defined as periods in which precipitation was absent for at least three consecutive days. All water samples were taken from the main streams including all tributaries; surface water ($n = 113$), spring water ($n = 46$), and ice ($n = 3$) as shown in Figure 3 during dry conditions. Every 200 m along the flowing stream channel, electrical conductivity (EC) and temperature (°C) were measured *in-situ* using a WTW LF340 series conductivity meter. A volume of 2 ml was collected in a glass bottle (PTFE/silicone septa) for stable isotopic analysis ($\delta^{18}O$, $\delta^{2}H$) and filled to the top to prevent evaporation. Every 400 m, two polyethylene bottles containing 25 ml water samples were filtered for major anions (Cl^-, SO_4^{2-}) and cations (Ca^{2+}, Mg^{2+}, Na^+, K^+) analysis. The latter bottle was previously prepared for preservation by adding a drop of nitric acid (HNO_3). All vials were kept in a cooling box at 1 – 5 °C. Ice samples were taken at the foot of the glacier at three different depths: 10, 20 and 30 cm.

Additional samples were also analysed for SiO_2 using the 8185 method of Silicomolybdate using a Hach DR890 Portable Spectrophotometer and for HCO_3^- using a Hach Digital Titrator (HACH 2014). Additional information such as weather conditions, GPS coordinates and a description of the sampling site was also recorded.

During wet conditions

During rainfall events, the sampling of the surface water and precipitation was undertaken only at the

outlet of the catchment at Humboldt Station for rainfall-runoff analyses. Surface water samples were collected with a frequency of 15–20 min at three main stages: (i) Pre-event, samples taken before the peak of the rainfall event ($n = 3$); (ii) Event, samples taken during the rainfall event ($n = 14$); and (iii) Post-event, samples taken after the peak of the rainfall event ($n = 12$).

Rainfall samples were collected using a self made device that consists of a funnel (diameter 140 mm) with a micro filter at the neck level joined to a drip chamber and to a 60 cm PVC tubing connected at the end to a rigid needle (3.8 cm, 28 G) embedded in rubber cork of a polyethylene vacuum packed bottle (1 L). One device was used per rainfall event, with the sample extracted immediately after or during the event following the procedure of the IAEA (IAEA/GNIP 2014).

All samples were analysed for major anions, cations and stable isotopes using the same procedure as described above in section *During dry conditions* and SiO_2, EC and temperature were measured *in-situ*.

Laboratory methods

Oxygen and hydrogen isotopic values, expressed in ‰ in relation to the Vienna Standard Mean Ocean Water (VSMOW), were measured using the Liquid-Water Isotope Analyzer (LGR DLT-100, precision <0.3‰ for $^{18}O/^{16}O$ and <1.0‰ for $^{2}H/^{1}H$). The samples for major cations were determined by mass spectrometry using the Thermo Fisher Scientific XSeries 2 ICP-MS (limit of quantification ~2 ppb). Anions were analysed by using ion chromatograph Dionex ICS-1000 (limit of quantification 2000 ppb). All analyses were performed following quality assurance and control procedures of the laboratory at UNESCO-IHE, Delft, the Netherlands.

Data analysis

Spatial hydrochemical characterization

The dispersion of sample measurements was plotted and the mean was computed for the different runoff sources, e.g. ice, precipitation, surface water and spring water (shallow and deep subsurface flow). Further analysis was done in the groups with a large dispersion: surface water and spring water. For surface water, the samples were divided in catchment and subcatchment level (Figure 3) for a detailed analysis to identify the origin of the variation of its concentration and to give more confidence intervals in the results. One-way ANOVA test was used to determine statistically significant differences ($P < 0.05$) among group means. Tukey multiple comparisons used as post-hoc tests after significant *t*-tests, are indicated by lowercase letters on top of each boxplot. For spring water, the samples were divided based on their geological background (Figure 1d). The same approach of checking dispersion and mean comparison was carried out.

Flow routing and contribution

Tracers enabled the identification not only of the runoff sources but also the quantity they contribute to the river flow. We applied the mass-balance approach from downstream to upstream to calculate the discharge when two streams met at the confluence point (Eqs. (1) and (2))

$$Q_T = Q_1 + Q_2 \quad (1)$$

$$C_T\ Q_T = C_1\ Q_1 + C_2\ Q_2 \quad (2)$$

where Q_T is the total runoff, Q_1, Q_2 are the runoff components in m^3/s and C_T, C_1, and C_2 are the concentrations of total runoff, and of the runoff components in mg/l or ‰. To assess the flow routing and contribution along the main rivers and tributaries in the catchment, concentrations were plotted against distance from the outlet.

End member mixing analysis (EMMA) and hydrograph separation

An End Member Mixing Analysis (EMMA) based on the method described by Christophersen and Hooper (1992) was carried out using the water quality parameters obtained. Mixing diagrams of EC (μS/cm), SiO_2 (mg/l), Cl^- (mg/l), SO_4^{2-}(mg/l), Na^+(mg/l), Mg^{2+}(mg/l), K^+(mg/l), Ca^{2+}(mg/l), and δ^2H and $\delta^{18}O$ (‰VSMOW) were created first to test their suitability as tracers for the hydrograph separation. In addition, these parameters were plotted against discharge to observe the dilution behaviour and hysteresis. Principal Component Analysis (PCA) was carried out on the above-mentioned parameters using R statistical software (R Development Core Team 2007) to indicate that two principal components explained at least 90% of the data variability and leading to a three component hydrograph separation. Isotope and hydrochemical data were combined with discharge data taken at the outlet of the basin to perform three-component hydrograph separations based on steady state mass balance equations and hydrograph separation assumptions (Pearce et al. 1986; Buttle 1994; Uhlenbrook et al. 2002). A third runoff component was included in Equations 1 and 2 to calculate three-component hydrograph separations for the total runoff (Q_T) (Eq. (3)):

$$C_T\ Q_T = C_1\ Q_1 + C_2\ Q_2 + C_3\ Q_3 \quad (3)$$

Rainfall characteristics, including duration, total rain, maximum and average intensity were estimated for the rain events. A rainfall event was defined as a rainfall occurrence with rainfall intensity greater

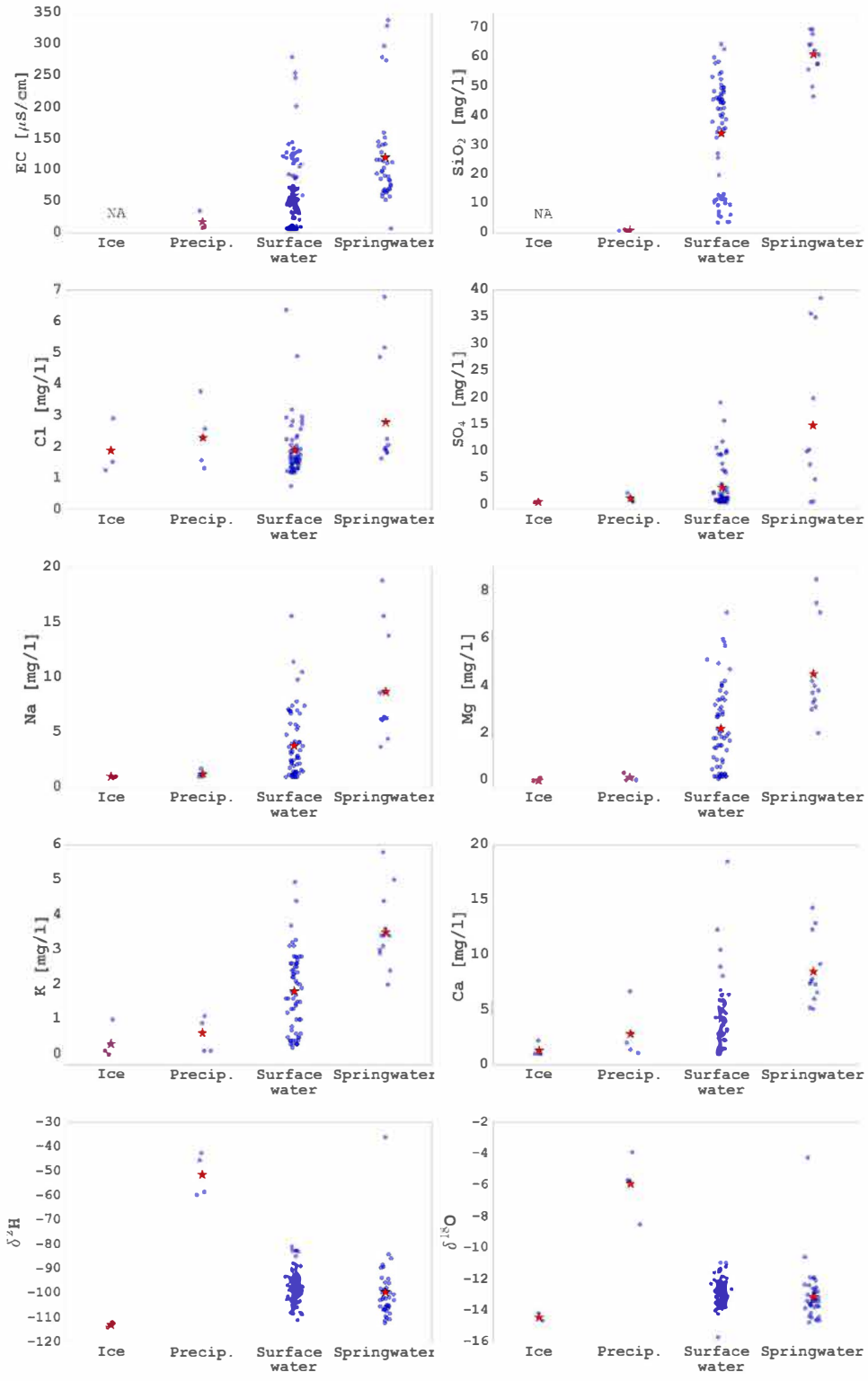

Figure 4. Chemical components and stable isotopes of water samples within the Los Crespos-Humboldt basin of different runoff sources (Ice, Precipitation, Surface and Spring water). The blue dots represent the samples and the red star the mean values. NA = samples are not available.

than 1 mm/hr, and intermittence less than four hours. Peak flow, water depth, and time to peak were determined for each event.

Analytical and tracer end-member uncertainties were accounted for the hydrograph separation and quantification of the runoff components based on a Gaussian error propagation technique with 70% confidence interval (Eq. (4)) (Genereux 1998):

$$W = \left\{ \left[\frac{\partial y}{\partial x_1} Wx_1 \right]^2 + \left[\frac{\partial y}{\partial x_2} Wx_2 \right]^2 + \ldots + \left[\frac{\partial y}{\partial x_n} Wx_s \right]^2 \right\}^{\frac{1}{2}} \quad (4)$$

where W is the uncertainty of the each runoff component in %, Wx_1x_2 are the standard deviations of each end-member, Wx_s is the analytical uncertainty

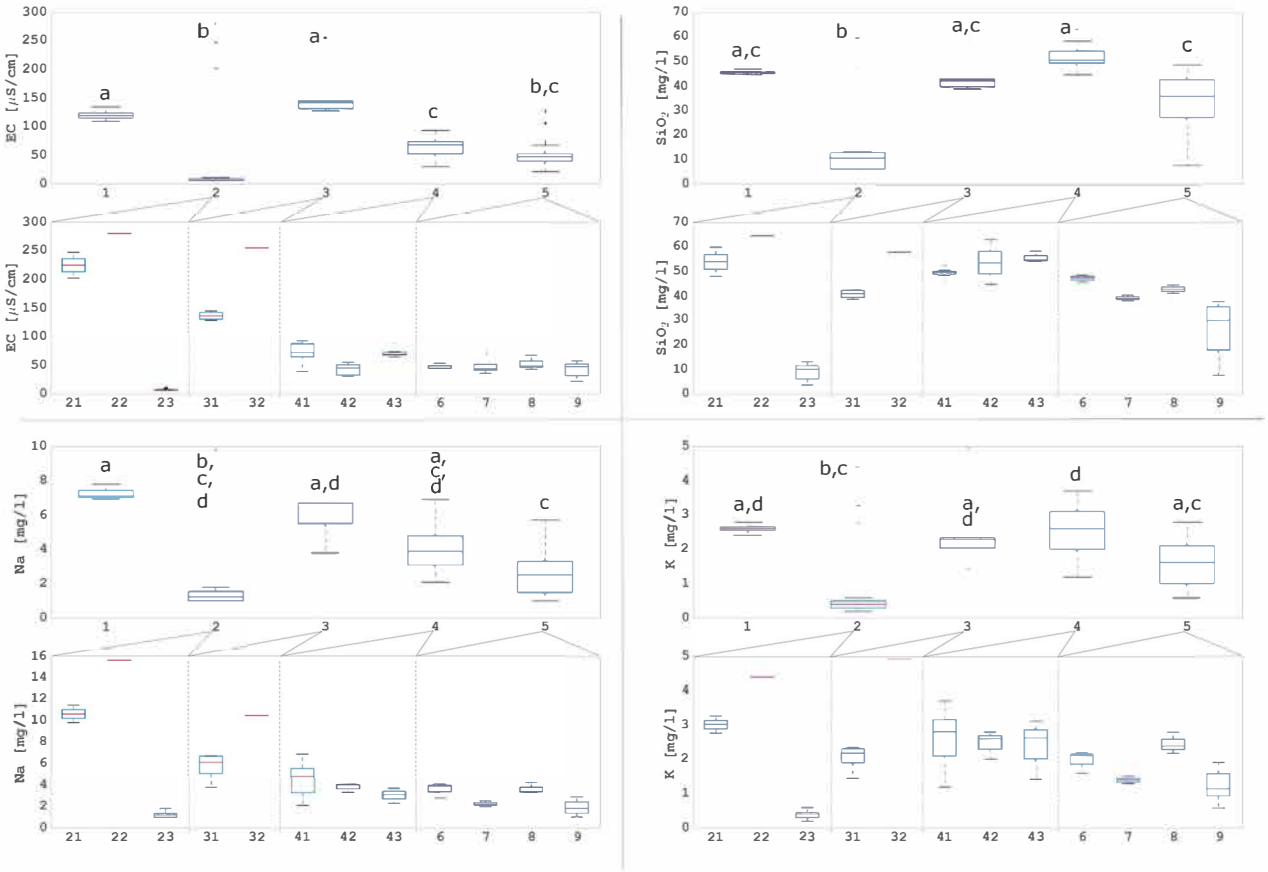

Figure 5. Major ions and EC values of water samples from surface water within the Los Crespos-Humboldt basin, analyzed per catchment and subcatchment. Lowercase letters indicate significant differences among catchments ($P \leq 0.05$), according to Tukey's test.

and $\frac{\partial y}{\partial x}$ are the uncertainties of the runoff component average contribution regarding the tracer concentrations.

Results

Hydrochemical catchment characterization

The location, main characteristics and chemical concentrations of all samples are shown in Table A1 in the supplemental material section. SiO_2, Na^+, K^+ and stable isotopes (δ^2H and $\delta^{18}O$) gave a first glimpse of the composition of these groups by showing such differences amongst all groups (Figure 4). Major ions and EC values in Ice and Precipitation showed lower values in comparison to surface water and spring water samples. These two last runoff sources require a distinctive classification to give more informative results and therefore those were disaggregated and grouped per subcatchment and per geological background, respectively.

Surface runoff – subcatchment analysis

The major ions (Na^+, K^+), SiO_2 and EC values from the subcatchments 41, 42, 43, 6, 7, 8 and 9 exhibited no clear contrasting patterns among them, thus can be considered as a single group (Figure 5). These subcatchments belong to catchments 4 and 5 which lie in a highly vegetated side of the catchment. Whereas subcatchment 21, 22 and 23 that belong to catchment 2 exhibited very distinctive patterns ($p \leq 0.05$) and therefore should remain grouped separately (Figure 5). All major cations showed significantly lower values of concentrations for subcatchment 23, thus demonstrating a unique hydrochemical characteristic of streams derived from glacier components. Subcatchments 31 and 32 showed different concentrations between them; however, their low is very low compared to the contributions from the other subcatchments.

Spring water – geological background analysis

Spring water samples that come from the Lahar Rojo (LaRo) formation showed distinctive higher concentrations in most of the major ions and EC values; whilst stable isotopes did not show specific patterns (Figure 6). The rest of the geological formations showed different concentration ranges that could not be tested for significance due to the lack of samples for specific major cations.

Flow paths and contribution

Distance to the outlet and elevation were highly correlated ($P < 0.001$) and assumed to have a linear response despite the weather conditions which can

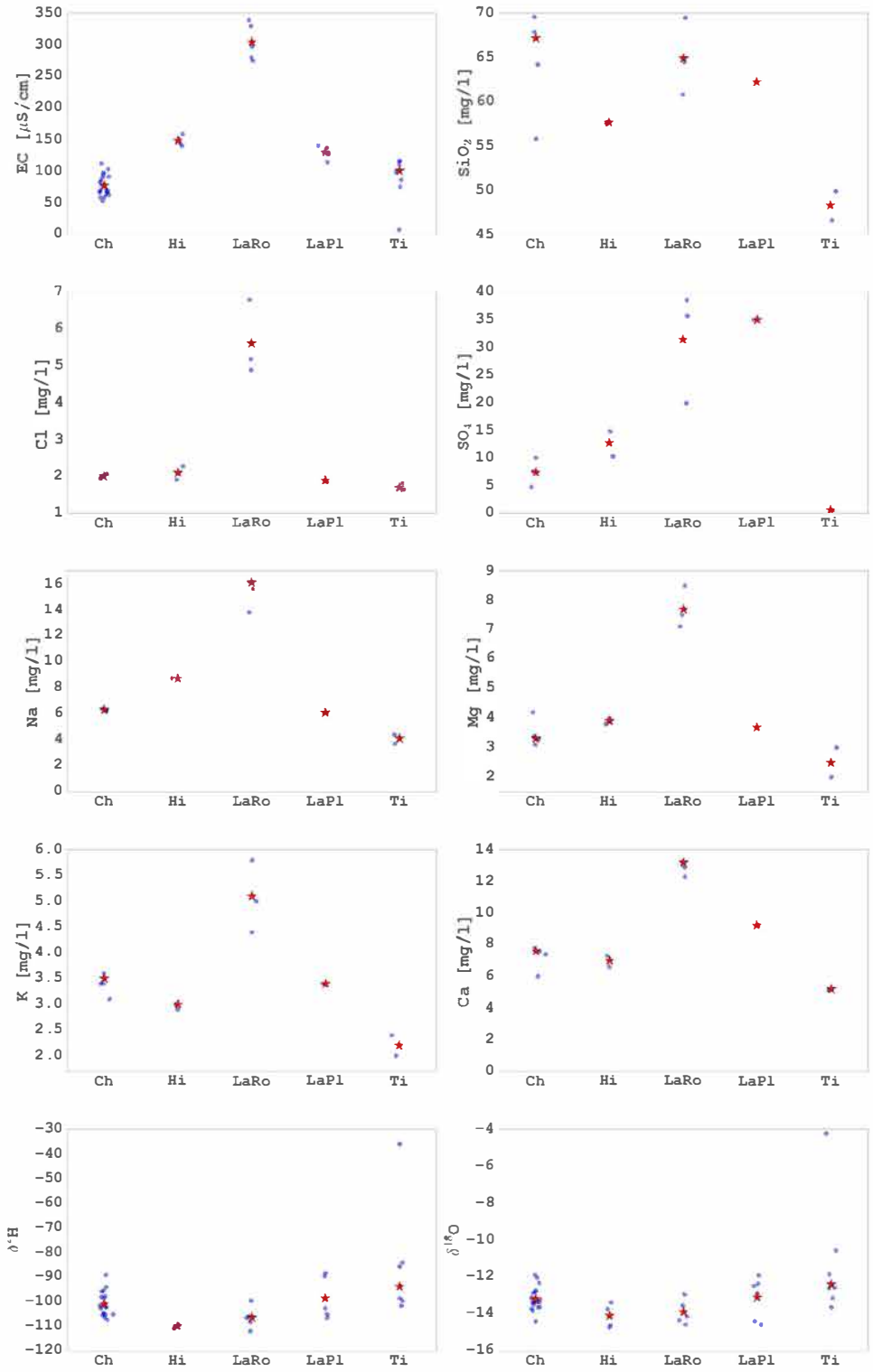

Figure 6. Chemical components and stable isotopes of spring water samples within the Los Crespos-Humboldt basin, analyzed per geological background (Ch = Chacana volcanic rocks, Hi = Hialina lava, LaRo = Lahar Rojo, LaPl = Lavas Pleistocene, Ti = Tillite late ice age).

differ at different locations within this high altitudinal mountain ecosystem. A distance to the outlet was selected to display the effect of surface water within the subcatchment and the confluence with other tributaries along the way to the outlet (Figure 7). The major ions and EC values showed a significant spatial variability and evidently separate two contrasting groups: surface water directly coming from the melting of the glacier (subcatchment 23) and the surface water that comes from the *páramo* vegetated areas (subcatchments 41, 42, 43, 6, 7, 8, 9). It should be noted that subcatchment 9 starts also with a small contribution of glacier but most of the water comes from the *páramo* vegetated areas. The high EC concentration values of subcatchments 22 and 31 are due to a considerable amount of

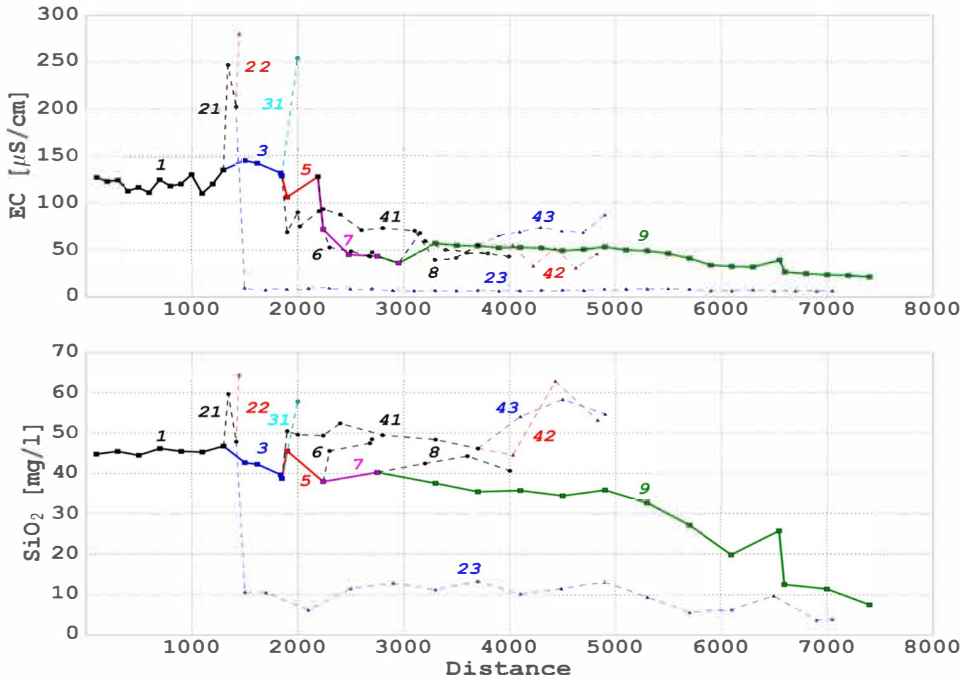

Figure 7. Chemical components of surface water samples within the Los Crespos-Humboldt basin, analyzed by distance to the outlet, numbers indicate subcatchment group. The thick solid line represents the main stream and dashed lines are the tributaries.

spring water contribution to the main channel as well as the small variations displayed among samples within the same subcatchments.

An initial estimation of the flow percentages during rainless periods was derived with EC, stable isotopes, and major ions independently. The flow path estimations for major ions were not considered because the concentrations and/or differences were too low thus giving unrealistic estimations for the subcatchments. Thus, EC values and stable isotopes were used to estimate the contribution of water from the glacier component, which was of 21% for EC, 14% for δ^2H and 15% for δ^{18}O during the sampling campaign on July 4–7, 2014. Likewise, the percentages of flow that comes from the páramo vegetated areas are 52% for EC, 71% for δ^2H and 78% for δ^{18}O, the remaining percentages come from small streams that join the main stream close to the outlet.

Water sources isotopic signatures

The sampling during the rainfall events corresponds to low-medium intensity rain and it was considered as representative for rainfall-runoff evaluation (Table A2 in supplemental material section). The duration of the event was 12 hours with a maximum intensity of 0.3 mm/h and an average intensity of 0.18 mm/h. Isotope composition for all samples in the catchment is shown in Figure 8. The Local Mean Water Line (LMWL) corresponds to the Izobamba station (0.37°S, 78.55°W), which lies nearby the location where the samples were taken (0.5°S, 78.18°W). Precipitation ranged from −8.5 to −3.9 ‰ for δ^{18}O and from −59.5 to −42.4 ‰ for δ^2H. Ice samples have a lighter isotopic signature, the lightest value corresponds to a 30 cm-depth sample, followed by a 20 cm-depth sample and the slightly enriched value belongs to the 10 cm-depth sample. The samples were clustered in such a way that the isotopic signature of the main river and tributaries that come from the *páramo* component were clearly identifiable, along with the glacier component. The signature of the surface water samples from the *páramo* component shows a relatively lighter or more depleted value of stable isotopes in comparison to the signature of the surface water samples from the glacier component, which are heavier or enriched. Signature from the surface water *páramo* showed a wide range of isotopic composition from −14.2 to −12.5 ‰ for δ^{18}O and from −108.6 to −95.3 ‰ for δ^2H. Likewise, the isotopic composition of surface water from glacier ranges from −13.4 to −12.3 ‰ for δ^{18}O and from −97.4 to −87.6 ‰ for δ^2H.

Hydrograph separation

Mixing plots were derived with all possible permutations of the small set of parameters (EC, SiO_2, Na^+, K^+, δ^{18}O, and δ^2H). Three main components were considered: precipitation, glacier and *páramo*, each of which has its own chemical signature and serves as a vertex of a triangle that defines the boundaries of the event runoff concentrations. EC and stable isotopes (δ^{18}O, and δ^2H) were identified as conservative tracers that characterize the end-member

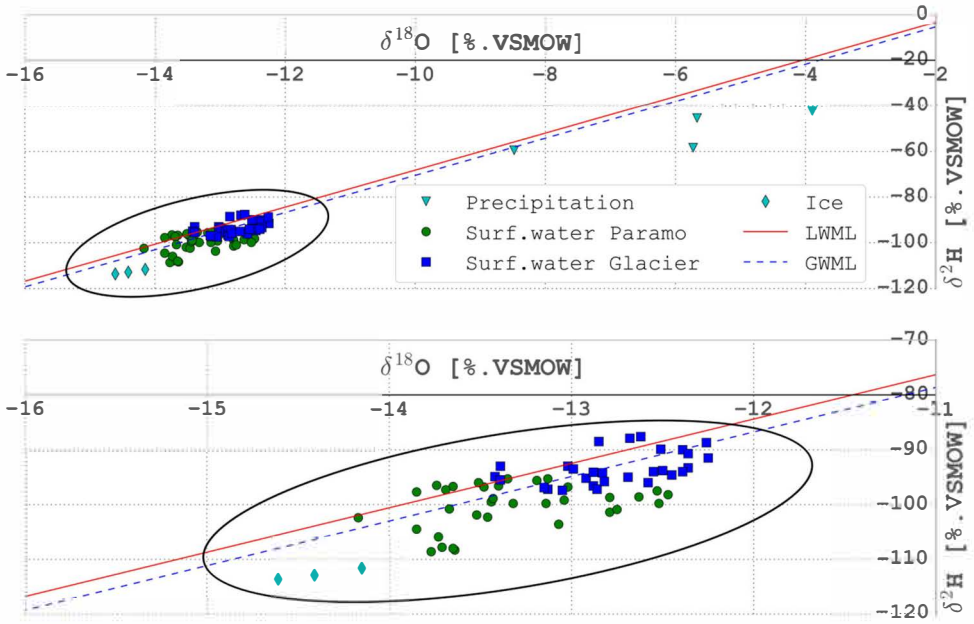

Figure 8. Stable isotope compositions of precipitation, surface water, and ice. Global Meteoric Water Line (GMWL): $\partial^2H = 8.13 \times \partial^{18}O + 10.8$ ‰ (Source: Rozanski et al. 1993). Local Mean Water Line (LMWL) for Izobamba: $\partial^2H = 8.1 \times \partial^{18}O + 12.8$ ‰ (Source: IAEA, 2016).

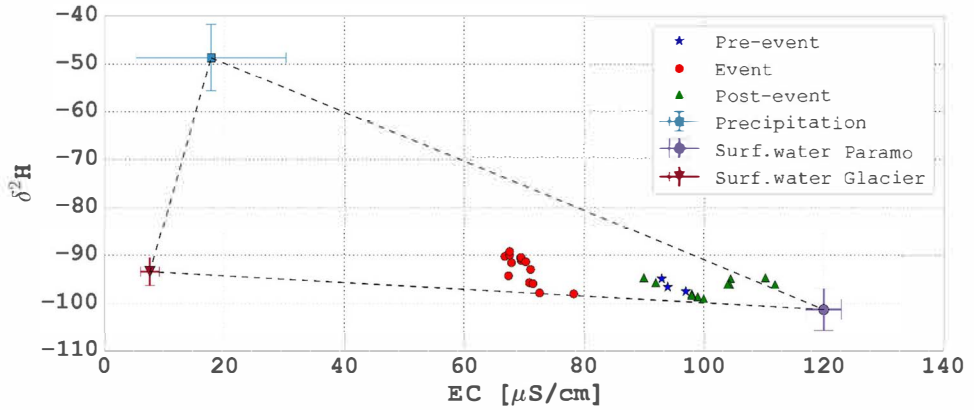

Figure 9. Mixing diagram showing stream water evolution and end-member EC and stable isotopes δ^2H.

concentrations represented by precipitation, glacier and *páramo* runoff (Figure 9). Most concentration points of the event water were located between the surface runoff from glacier and *páramo*. The mixing plot shows the evolution of the stream water before (pre-event), during (event) and after (post-event) the event. The discharge started with EC values of around 95 µs/cm, decreasing to an average of 70 µs/cm during the event and rising up to 105 µs/cm after 12 hours of the event. During the event the water samples concentration show slightly heavier isotope values.

The three-component hydrograph separation based on EC and δ^2H concentrations quantified the relative contribution of precipitation, glacier and *páramo* to the total flow. During the event, the total discharge was composed of 8% precipitation, 41% flow from glacier and 51% flow from the *páramo* component (Figure 10). The glacier component was the first to rise; the precipitation and *páramo* components have the maximum contribution during the peak time of the discharge. The rising limb mainly comprised similar contributions from glacier and *páramo* components and to a lesser extent by precipitation, whilst during the recession limb the contribution of precipitation increased. After the event runoff, there was still contribution from the *páramo* component while the contribution from the glacier decreased gradually as shown in Figure 10.

Discussion

Spatial hydrochemical analysis and suitable tracers

Silica (SiO_2) and EC were proved to be appropriate tracers to separate the main groups of runoff sources (precipitation, surface and spring water);

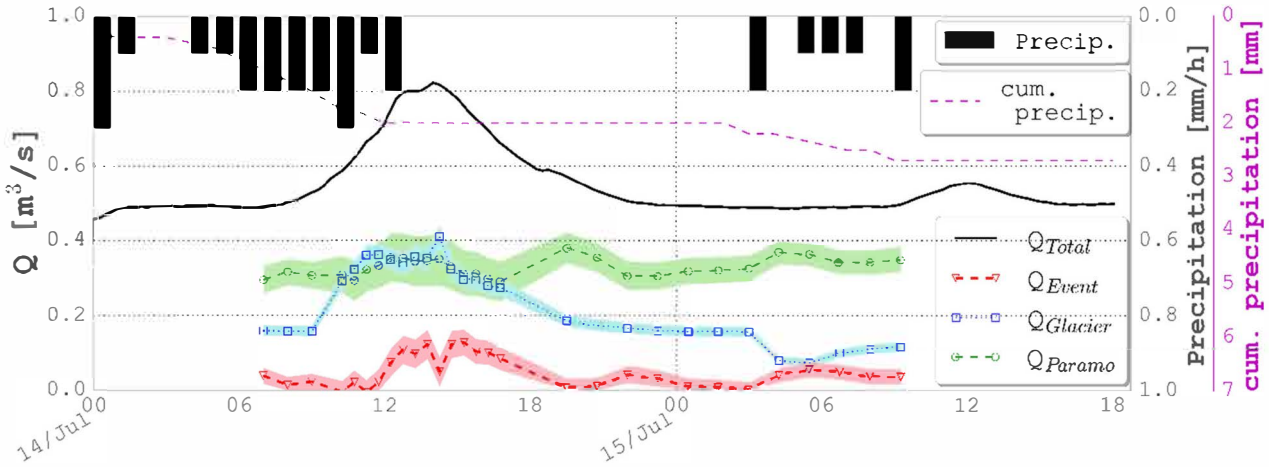

Figure 10. Three-component hydrograph separation, contribution of Glacier ($Q_{Glacier}$), *Páramo* (Q_{Paramo}) and event (Q_{Event}) to stream runoff based on the EMMA using EC and δ^2H as tracers for 14 July event. Colored area shows the estimated error propagation of the components.

whereas all major ions did not show clear difference between surface and spring water. In all cases, the spring water displayed higher values with large variations; this suggests that some runoff could originate from deeper sources, from fissures and fractures in the rock, where longer residence and contact times have increased the ion concentrations. However, attention should be paid to the outliers, which provide clear evidence of meltwater resurgence from the glacier. The latter confirms the meltwater infiltration during a study of the influence of the glacier on the water levels in the same catchment (Cauvy-Fraunié et al. 2013). Unfortunately, it is very difficult to crosscheck the water chemistry with the water signatures from the stable isotopes since they could be altered as a consequence of the strong influence of bedrock substrates, elevation and manifold underground processes (Nelson et al. 2011).

The analysis of surface water per subcatchment identified two distinctive groups, the samples from subcatchments 4 and 5 were pooled together and defined as the *páramo* component. Similarly, samples from subcatchment 23 were defined as the Glacier component since that was the stream that exclusively carried water from the melting glacier. However, during dry conditions in the diurnal cycle the contribution of the glacier might: a) increase as a consequence of the melting of the glacier due to the strong shortwave radiation especially in the low part of the glacier, and b) decrease as consequence of sublimation of the glacier due to high wind velocities (Favier et al. 2004).

EC, SiO_2, Na^+ and K^+ were appropriate tracers that displayed the significant difference between the glacier and the *páramo* component. The landscape played an important role influencing the hydrochemical composition of the surface water, as confirmed by the analysis of its distance to the outlet. The latter revealed the contribution of the spring water to the stream by showing changes in the concentration of the different tracers along each subcatchment and the shift in concentration while joining other subcatchments.

The stable isotopes ($\delta^{18}O$ and δ^2H) proved to be appropriate tracers to distinguish between precipitation and ice samples; however, they were unable to clearly distinguish between surface and spring water sources. This could be partially related to the mixing of surface water samples that were taken along the streams encompassing a combination of surface and spring water. Large variations in the stable isotopes could also be associated with the undetermined quantification of shallow and deep subsurface flow. The relative distance of the ice samples to the LMWL and GMWL curves are most likely due to evaporative losses during the melting as evidenced by the surplus of headspace within the vial. The comparatively higher concentrations in silica and the cations (Ca^{2+}, Mg^{2+}, Na^+, K^+) in spring water should be considered as indicators for water from deeper soil layers in study areas comparable to this one. These results strengthen the assumption that most of the spring water comes from a groundwater source; nevertheless, the discrimination among groundwater, shallow and deeper subsurface flows are subjects of further analysis which lies outside the scope of this study.

Catchment geology and weathering processes

Surface water samples obtained near the glacier and moraines formations (upper section of catchment 2) contain low EC (mean of 7.5 µS/cm) and silica concentrations (mean 9 mg/l), as well as other ions (Figure 5). Most of the spring water samples showed

silica concentrations of 55 to 70 mg/l; while the samples that correspond to the type of geology Tillita showed concentrations between 45 and 50 mg/l. In most of the cases, the latter type of geology consists of impermeable tough layers that have a shallow water table (Cuesta et al. 2013) and thus could easily get in contact with the subsurface flow and experience a dilution effect. Catchment 1, where the Hialiana lava formation is dominant, shows higher EC (mean: 149 µS/cm) and silica concentrations (mean: 48 mg/l). The Hialiana lava formation is dominant in catchment 1. This area is rich in olivine, plagioclase and quartz. Although quartz is highly resistant to weathering processes, olivines are known for decomposing faster (Goldich 1938; Appelo and Postma 2005). The weathering of these minerals results in increased contents of silica, bicarbonates, and cations in the water. Sodium is also derived from weathering of plagioclase materials. Catchment 1 contains the highest sodium concentrations (mean: 7.5 mg/l) as shown in Figure 5. The lavas Pleistocene are dominant in catchment 4. These are characteristic for also their high silica content (mean: 52 mg/l), but as opposed to the Hialina lava, they contain lower sodium concentrations (mean: 4 mg/l). Magnesium is evidence of weathering of pyroxenes and amphiboles. Catchment 4 displays a wider range of magnesium concentrations from 1.4 to 5.7 mg/l. For both catchments 1 and 4, calcium is known to be released with the weathering of ambhiboles and pyroxenes. These weathering processes may also result in the precipitation of carbonates and clay minerals. Surface water samples from the Lahar Rojo formation did not show the high ionic content expected as observed in the groundwater samples. Figure 6 shows the high concentrations observed in the Lahar Rojo section. The high clay content in this formation explains the high observed ionic content found in the groundwater samples. In catchments 5,6,7,8,9, the dominant formations are glacial fluvial sediments, tillites, and lava and breccia. These sediment deposits have lower electrical conductivities thus lower ionic content, but a wide range in silica concentrations. Their low ionic content is explained by the source of these materials which comes from the glacial debris.

Quantifying the contribution to event runoff

Separation of the contribution of each runoff component was challenging. The contributions may vary to an unknown amount due to unidentified layers and/or fissured and fractured rocks from which spring water originates. The contribution from the *páramo* is a result from the mixing between surface runoff, soil water, shallow surface flow and groundwater as evidenced in other small head watersheds (Marechal et al. 2013). Nevertheless, since the water sampled in the rivers took into account the contribution of spring water, our main objective remains in the quantification of the relative contribution from glacier and *páramo* and their evolution with time as the main components for the total runoff at the outlet of the catchment.

The isotopic composition of rainfall and their relative distance to the LMWL propose a possible evaporation effect that occur when raindrops fall in a warm atmosphere. This is suggested by the values of deuterium excess less than 10‰ in all precipitation samples. The first raindrops are usually more isotopically enriched (Gat and Matsui 1991). In addition, the conditions between the Izobamba station (3059 m a.s.l.), where the LMWL was recorded, and the Humboldt station (4010 m a.s.l.), where the samples were taken, are slightly different. The precipitation registered at Izobamba station is around 1400 mm/yr compared to 800 mm/yr at Humboldt station. The Andean Region is dominated by the elevation effect and could explain locally the significant deviations from the LWML. For the specific case of precipitation, further research on rainfall events at this location should be done to check for possible re-evaporation processes and contributions of different water vapour sources that might occur taking into account inter and intra event variability in the hydrological process. Spring water signature has a wide range; those that showed heavier isotopic composition could be associated to precipitation, wetland or shallow subsurface recharge. Conversely, those with depleted compositions could be linked to deeper subsurface layers, and moreover, the high EC concentrations imply that the water could have been stored for a longer period of time and it also depends on the type of rocks where mineralization is very fast. During the event, the water samples either contained heavier isotopes that came from the rain, or could be associated with wetlands/open waters or shallow subsurface flow (from previous rainfall events), and also with contributions from the saturated zone, which can be highly dynamic. The challenge to separate the runoff components in this catchment was investigated in earlier studies (Mena 2010) that estimated an average contribution of 45% of the glacier component, slightly above the estimation of 41% reported in the present study. Natural *páramo* can vary around 50 to 70%, while this study reported around 51% (± 5% uncertainty). The remaining contribution from the event can be attributed to direct superficial runoff.

A representative end-member mixing analysis was carried out with three main components: event,

glacier and *páramo* as justified earlier. Some of the monitored event flow samples were not fully confined within the triangles, which might increase the uncertainty in the evaluated event.

In order to overcome the limitations of non-conservative behaviour of major ions, the application of stable isotopes for the hydrograph separation was preferred, a technique used commonly in tropical and subtropical areas (Elsenbeer 2001; Goller et al. 2005; Mul et al. 2008; Klaus and McDonnell 2013). In the present work, a plausible approach was the combination of EC and δ^2H that demonstrated a clear separation of the three distinctive components: event, glacier and *páramo* likewise stated by Mena (2010). It is important to realize that these types of tropical Andean catchments have high spatial variability of precipitation (Buytaert et al. 2006b; Celleri et al. 2007; Buytaert and Beven 2011) due to orographic effects, which to a certain extent can influence and might mislead the quantification of the contribution of this component.

Based on the hydrograph separation, the contribution of the glacier component during the rainfall event increases at a faster rate. This is mainly attributed to the lack of water retention in that subcatchment and yet the riparian area consists mainly of boulders, rocks and large soil particles that drain rapidly with a very low water retention capability. Conversely, in the *páramo* region there are several zones with less steep slopes that are hydrologically disconnected due to the irregular terrain (Buytaert and Beven 2011). Yet, they behave as floodplains, swamps and wetlands that dissipate the stream energy and buffer the peak flow at the outlet, contrary to what was found in a similar study by Buytaert et al. (2010). The soils of the riparian zone in the *páramo* subcatchments comprise smaller soil particles that are poor in percolation, thus offer a high water-holding capacity (Minaya et al. 2016) and consequently high water attenuation (Buytaert and Beven 2011). Equally important is the interception of rainfall, which is the first process in a rainfall-runoff event. This interception particularly in the tussock vegetation should not be neglected and might contribute to a longer lag time during rainfall events and an increased recharge of water into the soil in these high altitude ecosystems (Buytaert and Beven 2009; Janeau et al. 2015).

Conclusions

This study estimated relative contributions of the main runoff components during dry and wet conditions from a combined glacier and *páramos* catchment. It provided valuable information on the origin of water and the hydrological and hydrochemical characteristics of the water cycle in this high mountainous region. This runoff ratio cannot be assumed to be maintained in the future because it is linked to future climate and land-use drivers. Moreover, adequate water resource management should include the protection of the *páramos* as reservoirs of water in the highlands since they are major contributors to runoff.

Rainfall events were monitored with medium intensity and the runoff generation patterns are in line with the expected dynamics within this catchment. The high runoff contribution of the glacier component during rain events remains valid. Two sources with clear evidence of resurgence of meltwater from the glacier were identified, characterized consistently by low values of EC. It should be noted that during rainless times, there might be a higher variability due to the diurnal cycle and contribution of melt water due to the exposure to solar radiation. Therefore, the effect of temporal resolution needs to be further studied since these streams depend on the glacier influence. Certainly, long-term analysis will contribute to a better understanding of the dependency of runoff generation on soil moisture and vegetation interaction.

This study focuses on the spatial representation of the main runoff components. Further investigation is recommended with respect to the separation of shallow and deep subsurface flows. Moreover, the clustering of groundwater movement into a single group as 'spring water' offers further scope for investigation. The lack of soil moisture measurements and assumptions of the permanently saturated zones added uncertainty to the quantification of the subsurface processes that regulate the contribution of surface runoff. Despite these limitations and uncertainties, the combination of stable isotopes and geochemical tracers improved the understanding of runoff processes in this combined glacier and *páramo* catchment in the Ecuadorian Andean region, for which no runoff investigations were available before.

Acknowledgements

Other institutions that also cooperated in the provision of key information and data are EPMAPS (Empresa Pública Metropolitana de Agua Potable y Saneamiento de Quito), EPN (Escuela Politécnica Nacional), INAMHI (Instituto Nacional de Meteorología e Hidrología), INIGEMM (Instituto Nacional de Investigación Geológico Minero Metalúrgico). The authors express their sincere gratitude to Fred Kruis, Ferdi Battes and Berend Lolkema for their assistance in the laboratory analysis. Thanks also to Aline Saraiva Okello, Lydia Cumiskey; and to Gareth Bird for proof reading the manuscript. The opinions expressed in this paper are those of the author(s) and do not necessarily reflect views of any of the Institutions named above.

Disclosure statement

No potential conflict of interest was reported by the authors.

Funding

Financial support came from SENESCYT (Secretaría Nacional de Educación Superior, Ciencia, Tecnología e Innovación) and from the Dutch Ministry of Foreign Affairs (DUPC program at UNESCO-IHE).

References

Alvarado C. 2009. Caracterización hidrogeológica de ls vertientes occidentales del volcán Antisana como parte de los estudios de los glaciares y páramos frente al cambio climático [Unpublished dissertation thesis]. Quito: Escuela de Ingeniería en Geología, Universidad Central del Ecuador.

Appelo CAJ, Postma D. 2005. Silicate weathering. Geochemistry, groundwater and pollution. 2nd ed., p. 375–414. Leiden, The Netherlands: Taylor & Francis.

Beniston M. 2003. Climatic change in mountain regions: A review of possible impacts. Clim Change. 59(1/2): 5–31.

Bernard B, Andrade D. 2011. Volcanes cuaternarios del ecuador continental. IG EPN Poster Informativo.

Bradley RS, Vuille M, Diaz HF, Vergara W. 2006. Climate change. Threats to water supplies in the tropical Andes. Science. 312(5781):1755–1756.

Brown LE, Milner AM, Hannah DM. 2010. Predicting river ecosystem response to glacial meltwater dynamic: a case study of quantitative water sourcing and glaciality index approaches. Aquat Sci. 72(3):325–334.

Buttle JM. 1994. Isotope hydrograph separations and rapid delivery of pre-event water from drainage basins. Prog Phys Geogr. 18(1):16–41.,

Buytaert W, Iniguez V, Celleri R, De Bievre B, Wyseure G, Deckers J. 2005b. Analysis of the water balance of small paramo catchments in south Ecuador. International Conference on Headwater Control VI: Hydrology, Ecology and Water Resources in Headwaters, Bergen, Norway, 20–23 June.

Buytaert W, Beven K. 2009. Regionalization as a learning process. Water Resour Res. 45(11):W11419.

Buytaert W, Beven K. 2011. Models as multiple working hypotheses: hydrological simulation of tropical alpine wetlands. Hydrol Process. 25(11):1784–1799.

Buytaert W, Celleri R, De Bievre B, Hofstede R, Cisneros F, Wyseure G, Deckers J. 2006a. Human impact on the hydrology of the Andean paramos. Earth Sci Rev. 79(1–2):53–72.

Buytaert W, Celleri R, Willems P, De Bievre B, Wyseure G. 2006b. Spatial and temporal rainfall variability in mountainous areas: a case study from the south Ecuadorian Andes. J Hydrol. 329(3–4):413–421.

Buytaert W, Deckers J, Wyseure G. 2005a. Description and classification of nonallophanic Andosols in south Ecuadorian alpine grasslands (páramo). Geomorphology. 73(3–4):207–221.

Buytaert W, Vuille M, Dewulf A, Urrutia R, Karmalkar A, Celleri R. 2010. Uncertainties in climate change projections and regional downscaling in the tropical Andes: implications for water resources management. Hydrol Earth Syst Sci. 14(7):1247–1258.

Cáceres B, Maisincho L, Taupin JD, Francou B, Cadier E, Delachaux F, Bucher R, Villacis M, Paredes D, Chazarin JP, et al. 2005. fes del Ecuador: Antizana y Carihauyrazo. Balance de masa, topografía, meteorología e hidrología, IRD/INAMHI/EMAAP, pp. 171, Quito.

Carrillo-Rojas G, Silva B, Córdova M, Célleri R, Bendix J. 2016. Dynamic mapping of evapotranspiration using an energy balance-based model over an andean páramo catchment of Southern Ecuador. Remote Sens. 8(2): 160–124.

Cauvy-Fraunié S, Condom T, Rabatel A, Villacis M, Jacobsen D, Dangles O. 2013. Techincal note: Glacial influence in tropical mountain hydrosystems evidenced by the diurnal cycle in water levels. Hydrol Earth Syst Sci. 17(12):4803–4816.

Celleri R, Feyen J. 2009. The hydrology of Tropical Andean ecosystems: importance, knowledge status, and perspectives. Int Mountain Soc. 29(4):350–355.

Celleri R, Willems P, Buytaert W, Feyen J. 2007. Spacetime variability of rainfall in the Paute basin. Hydrol Process. 21(24):3316–3327.

Christophersen N, Hooper RP. 1992. Multivariate-analysis of stream water chemical-data – the use of principal components-analysis for the end-member mixing problem. Water Resour Res. 28(1):99–107.

Condom T, Escobar M, Purkey D, Pouget JC, Suarez W, Ramos C, Apaestegui J, Tacsi A, Gomez J. 2012. Simulating the implications of glaciers' retreat for water management: a case study in the Rio Santa basin, Peru. Water Int. 37(4):442–459.

Crockford RH, Richardson DP. 2000. Partitioning of rainfall into throughfall, stemflow and interception: effect of forest type, ground cover and climate. Hydrol Process. 14(16–17):2903–2920.

Cuesta F, Sevink J, Llambí LD, De Bièvre B, Posner J. 2013. Avances en investigación para la conservación de los páramos andinos. Lima, Peru: CONDESAN.

Dahlke HE, Lyon SW, Jansson P, Karlin T, Rosqvist G. 2012. Isotopic investigation of runoff generation in a glacierized catchment in northern Sweden. Hydrol Process. 28(3):1383–1398.

Elsenbeer H. 2001. Hydrologic flowpaths in tropical rainforest soilscapes – a review. Hydrol Process. 15(10): 1751–1759.

Favier V, Coudrain A, Cadier E, Francou B, Ayabaca E, Maisincho L, Praderio E, Villacis M, Wagnon P. 2008. Evidence of groundwater flow on Antizana ice-covered volcano, Ecuador/Mise en évidence d'écoulements souterrains sur le volcan englacé Antizana, Equateur. Hydrolog Sci. 53(1):278–291.

Favier V, Wagnon P, Chazarin JP, Maisincho L, Coudrain A. 2004. One-year measurements of surface heat budget on the ablation zone of Antizana Glacier 5, Ecuadorian Andes. Geophys Res. 109:D18105.

Foot K, Morgan RPC. 2005. The role of leaf inclination, leaf orientation and plant canopy architecture in soil particle detachment by raindrops. Earth Surf Process Landforms. 30(12):1509–1520.

Gardi C, Angelini M, Barceló S, Comerma J, Cruz Gaistardo C, Encina Rojas A, Jones A, Krasilnikov P, Mendonça Santos Brefin ML, Montanarella L, et al. 2014.: Atlas de suelos de América Latina y el Caribe. In Europea C, ed., Luxembourg: Oficina de Publicaciones de la Unión Europea, L-2995, p. 176.

Gat JR, Matsui E. 1991. Evolution of the isotopic composition of atmospheric waters in the Mediterranean Sea area. J Geophys Res. 96(D7):13179–13188.
Genereux D. 1998. Quantifying uncertainty in tracer-based hydrograph separations. Water Resour Res. 34(4):915–919.
Goldich SS. 1938. A study in rock-weathering. J Geology. 46(1):17–58.
Goller R, Wilcke W, Leng MJ, Tobschall HJ, Wagner K, Valarezo C, Zech W. 2005. Tracing water paths through small catchments under a tropical montane rain forest in south Ecuador by an oxygen isotope approach. J. Hydrology. 308(1–4):67–80.
HACH. 2014. Silica, silicomolybdate HR method 8185, Powder Pillows. DOC316.53.01133. Edition 9. Loveland, USA: Hach Company/Hach Lange GmbH.
Hall M, Mothes P, Aguilar J, Bustillos J, Ramon P, Eissen JP, Monzier M, Robin C, Egred J, Militzer A, et al. 2012. Los peligros volcánicos asociados con el Antisana, in: Serie los peligros volcánicos en el Ecuador, No. 4, Corporación Editora Nacional/IG-EPN/IRD, Quito.
Hall M, Mothes P. 1999. La actividad volcánica del Holoceno en el Ecuador y Colombia Austral, Impedimento al desarrollo de las civilizaciones pasadas. In: Mothes P, editors. Actividad volcánica y pueblos precolombinos en el Ecuador. Quito, Ecuador: Editorial Abya Yala, p. 11–40.
Hall M, Mothes PA, Samaniego P, Militzer A, Beate B, Ramón P, Robin C. 2017. Antisana volcano: A representative andesitic volcano of the eastern cordillera of Ecuador: Petrography, chemistry, tephra and glacial stratigraphy. J South Am Earth Sci. 73:50–64.
Hofstede R, Coppus R, Mena-Vasconez P, Segarra P, Wolf J, Sevink J. 2002. El estado de conservacion de los paramos de pajonal en el Ecuador. Ecotropicos. 15: 3–18.
Huss M, Farinotti D, Bauder A, Funk M. 2008. MOdelling runoff from highly glacierized alpine drainage basins in a changing climate. Hydrol Process. 22(19):3888–3902.
IAEA/GNIP. 2014. Precipitation sampling guide, V2.02 September.
Janeau JL, Grellier S, Podwojewski P. 2015. Influence of rainfall interception by endemic plants versus short cycle crops on water infiltration in high altitude ecosystems of Ecuador. Hydrol Res. 46(6):1008–1018.
Jansky L, Ives JD, Furuyashiki K, Watanabe T. 2002. Global mountain research for sustainable development. Global Environ Change. 12(3):231–239.
Kaser G, Grosshauser M, Marzeion B. 2010. Contribution potential of glaciers to water availability in different climate regimes. Proc Natl Acad Sci U S A. 107(47): 20223–20227.
Kaser G, Osmaston H. 2002. Tropical glaciers. International Hydrology Series. Cambridge, England: Cambridge University Press.
Klaus J, McDonnell JJ. 2013. Hydrograph separation using stable isotopes: review and evaluation. J. Hydrology. 505:47–64.
Lo CP, Yeung AKW. 2007. Concept and techniques in geographic information systems. 2nd ed. Upper Saddle River, NJ: Prentice Hall.
Luteyn JL. 1999. Páramos, a checklist of plant diversity, geographical distribution and botanical literature. New York: New York Botanical Garden Press.
Madriñán S, Cortés AJ, Richardson JE. 2013. Páramo is the world's fastest evolving and coolest biodiversity hotspot. Front Genet. 4:192.
Marechal J, Ladouche B, Batiot-Guilhe C, Seidel J. 2013. Application of end-member mixing analysis to karst hydrogeology. San Francisco, CA: American Geophysical Union. Fall Meeting abstract #H23G-1356, 2013.
Mark DM. 1984. Automated detection of drainage networks from digital elevation models. Cartographica. 21(2–3):168–178.
Mena SP. 2010. Evolución de la dinámica de los escurrimientos en zonas de alta montaña: caso del Volcán Antisana [Unpublished dissertation, Thesis]. Facultad de Ingeniería Civil y Ambiental, Escuela Politécnica Nacional, Quito - Ecuador. http://bibdigital.epn.edu.ec/handle/15000/2503.
Minaya V, Corzo G, Romero-Saltos H, van der Kwast J, Lantinga E, Galarraga-Sanchez R, Mynett AE. 2016. Altitudinal analysis of carbon stocks in the Antisana *páramo*. JPECOL. 9(5):553–563.
Mul ML, Mutiibwa RK, Uhlenbrook S, Savenije HHG. 2008. Hydrograph separation using hydrochemical tracers in the Mankanya catchment, Tanzania. Phys Chem Earth. 33(1–2):151–156.
Munyaneza O, Wenninger J, Uhlenbrook S. 2012. Identification of runoff generation processes using hydrometric and tracer methods in a meso-scale catchment in Rwanda. Hydrol Earth Syst Sci. 16(7):1991–2004.
Nelson ML, Rhoades CC, Dwire KA. 2011. Influence of bedrock geology on water chemistry of slope wetlands and headwater streams in the southern Rocky Mountains. Wetlands. 31(2):251–261.
O'Callaghan JF, Mark DM. 1984. The extraction of drainage networks from digital elevation data. Comput Vis Graph Image Process. 28:328–344.
Pearce AJ, Stewart MK, Sklash MG. 1986. Storm runoff generation in humid headwater catchments 1. Where does the water come from? Water Resour Res. 22(8):1263–1272.
Poulenard J, Bartoli F, Burtin G. 2002. Shrinkage and drainage in aggregates of volcanic soils: a new approach combining mercury porosimetry and vacuum drying kinetics. Eur J Soil Sci. 53(4):563–574.
R Development Core Team. 2007. R: A language and environment for statistical computing. http://www.R-project.org/.
Roa-García MC, Brown S, Schreier H, Lavkulich LM. 2011. The role of land use and soils in regulating water flow in small headwater catchments of the Andes. Water Resour Res. 47:W05510.
Rozanski K, Araguás-Araguás L, Gonfiantini R. 1993. Isotopic patterns in modern global precipitation. Geophys Monogr Ser. 78:1–36.
Tarboton DG. 1997. A new method for the determination of flow directions and upslope areas in grid digital elevation models. Water Resour Res. 33(2):309–319.
Tonneijck FH. 2009. Volcanic ash soils in Andean ecosystems: unravelling organic matter distribution and stabilisation [PhD thesis]. Amsterdam: UvA-DARE Universiteit van Amsterdam.
Uhlenbrook S, Frey M, Leibundgut C, Maloszewski P. 2002. Hydrograph separations in a mesoscale mountainous basin at event and seasonal timescales. Water Resour Res. 38(6):31–1–31-14.
Villacis M, Vimeux F, Taupin JD. 2008. Analysis of the climate controls on the isotopic composition of

precipitation ($d^{18}O$) at Nuevo Rocafuerte, 74.5°W, 0.9°S, 250 m, Ecuador. C.R. Geoscience. 340(1):1–9.

Villacis M. 2008. Ressources en eau glaciaire dans les Andes d'Equateur en relation avec les variations du climat: le cas du volcan Antisana [PhD Thesis]. Montpellier, France: UniversitéMontpellier II.

Viviroli D, Archer DR, Buytaert W, Fowler G, Greenwood GB, Hamlet AF, Huang Y, Koboltschnig G, Litaor MI, López-Moreno JI, et al. 2011. Climate change and mountain water resources: overview and recommendations for research, management and policy. Hydrol Earth Syst Sci. 15(2):471–504.:

Vuille M, Bradley RS, Keimig F. 2000. Interannual climate variability in the Central Andes and its relation to tropical Pacific and Atlantic forcing. J Geophys Res. 105(D10):12447–12460.

Water Resources Programme. 2016. Global network of isotopes in precipitation. [accessed 2015, Dec 1]. http://www-naweb.iaea.org/napc/ih/IHS_resources_gnip.html.

Wenninger J, Uhlenbrook S, Lorentz S, Leibundgut C. 2008. Identification of runoff generation processes using combined hydrometric, tracer and geophysical methods in a headwater catchment in South Africa. Hydrol Sci J. 53(1):65–80.

Windhorst D, Waltz T, Timbe E, Frede HG, Breuer L. 2013. Impact of elevation and weather patterns on the isotopic composition of precipitation in a tropical montane rainforest. Hydrol Earth Syst Sci. 17(1):409–419.